Available online at www.sciencedirect.com
SCIENCE DIRECT®
Polymer 44 (2003) 7413–7425
polymer
www.elsevier.com/locate/polymer

Synthesis and dipole–dipole interaction-induced mesomorphic behavior of poly(oxyethylene)s containing (*n*-octylsulfonyl)alkylthiomethyl or (*n*-octylsulfonyl)alkylsulfonylmethyl side groups

Jong-Chan Lee[a,*], Se-Hui Han[a], Sang-Ho Cha[a], Soo-Young Park[b], B.L. Farmer[c]

[a]*School of Chemical Engineering, Seoul National University, Seoul 151-744, South Korea*
[b]*Department of Polymer Science, Kyungpook University, Daegu 702-701, South Korea*
[c]*Air Force Research Laboratory, Materials and Manufacturing Directorate, Wright-Patterson Air Force Base, OH 45433-7750, USA*

Received 25 February 2003; received in revised form 2 September 2003; accepted 12 September 2003

Abstract

Two series of ((*n*-octylsulfonyl)alkylthio)methyl-substituted poly(oxyethylene)s ($(-OCH_2CHR-)_n$, where $R = -CH_2S(CH_2)_MSO_2(CH_2)_8H$) (OTP-*M*, $M = 3, 4, 5, 6, 7, 9, 12$), and ((*n*-octylsulfonyl)alkylsulfonyl)methyl-substituted poly(oxyethylene) ($(-OCH_2CHR-)_n$, where $R = -CH_2SO_2-(CH_2)_MSO_2(CH_2)_8H$) (OSP-*M*, $M = 3, 4, 5, 6, 7, 9, 12$), were synthesized using polymer analogous reactions from poly(epichlorohydrin) to study the effect of dipole–dipole interactions of the sulfone groups (SO_2) on the ordered structures of the poly(oxyethylene) derivatives. The ordered phases of these polymers were studied using polarizing optical microscopy, X-ray diffraction, differential scanning calorimetry and IR spectroscopy. OTP-Ms and OSP-3 showed ordered phases originated from side chain crystallization, while OSP-Ms except OSP-3 showed liquid crystalline behavior. The poly(oxyethylene) derivatives with $M = 5, 6, 7$ had double-layer structures, while the polymers with $M = 3, 4, 9, 12$ had intercalating double-layer structures at room temperature. The layer structures of the poly(oxyethylene) derivatives were found to be affected by the positions of the side chain sulfone groups which can generate strong dipole–dipole interactions.
© 2003 Elsevier Ltd. All rights reserved.

Keywords: Poly(oxyethylene); Dipole–dipole interaction; Liquid crystalline polymer

1. Introduction

The preparation of self-ordering polymeric materials has attracted much attention due to the possible applications in electronic and biological materials [1–4]. Studies on the ordered structures of the polymers created by means of molecular interactions such as hydrogen bonding, ionic interactions, metal coordination, and hydrophilic and hydrophobic effects have been done intensively [5–9]. However, the ordered structure formation by dipole–dipole interactions between the polar groups in polymers has not been received much attention. There are several reports on the liquid crystalline and/or self-assembly behavior of aliphatic polymers containing sulfone groups in the main chain or in the side chain [10–13]. The liquid crystallinity of these polymers is very unusual since they do not contain any conventional mesogenic groups such as aromatic or aliphatic cyclic rings [14–16]. The ordered phases of such polymers have been ascribed to the very strong dipole–dipole interactions between the sulfone groups because the electrostatic interactions of the sulfone groups can create very stiff sections in the polymers. Strong interactions between sulfone groups are possible because the sulfone group has a very high dipole moment, for example dimethyl sulfone has a dipole moment of 4.49 Debye [17]. Since the liquid crystalline behavior of the aliphatic sulfone polymers is very unique, we believe that and the dipole–dipole interactions between the sulfone groups could be usefully applied for the formation of novel self-organizing structures.

This time we synthesized a series of ((*n*-octylsulfonyl)-alkylthio)methyl-substituted poly(oxyethylene)s and ((*n*-octylsulfonyl)alkylsulfonyl)methyl-substituted poly-(oxyethylene)s using polymer analogous reactions from atatic poly(epichlorohydrin) (Scheme 1). The amorphous

* Corresponding author. Tel.: +82-2-880-7070; fax: +82-2-888-1604.
E-mail address: jongchan@snu.ac.kr (J.C. Lee).

0032-3861/$ - see front matter © 2003 Elsevier Ltd. All rights reserved.
doi:10.1016/j.polymer.2003.09.030

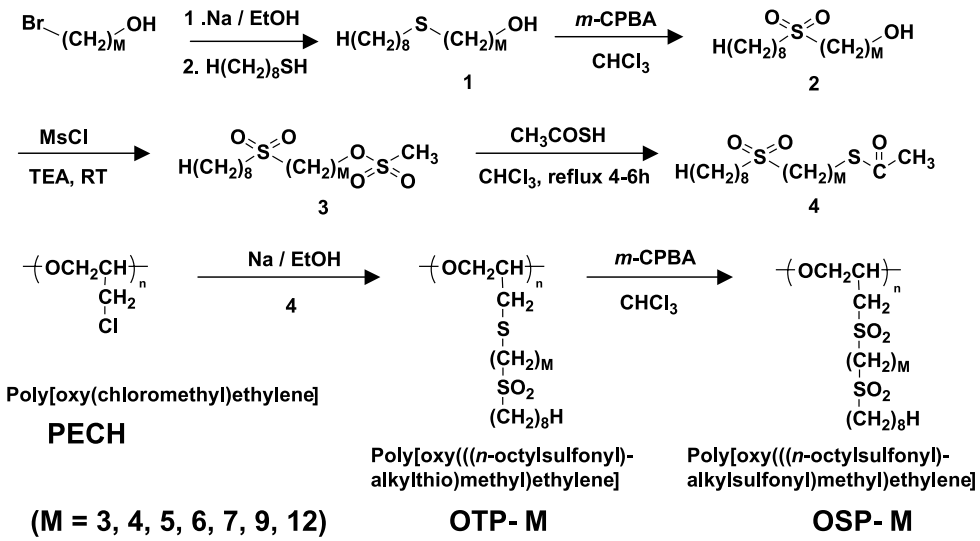

Scheme 1.

poly[oxy(chloromethyl)ethylene] (atactic configuration of the oxyethylene backbones) was intentionally used to study the ordered phases arisen from the side chains containing polar sulfone groups. The number of carbons, *M*, in the alky groups between the two sulfur containing groups was varied from 3 to 12 (Scheme 1) to study the effect of the spacer length and the position of the sulfone groups on the ordered phases and structures. The octyl group was used as a tail group because we had found that poly(oxyethylene)s with eight carbons in the side tail part have ordered phases [18].

2. Experimental section

2.1. Materials

N,*N*-Dimethylacetamide (DMAc) and absolute ethanol were dried over molecular sieves (4 Å). All other reagents including poly[oxy(chloromethyl)ethylene] (Hydrin H®, Zeon Chemical Inc.) (PECH) and solvents were used as received.

2.2. Instrumentations

NMR spectra were obtained on JEOL JNM-LA 300 spectrometer at 300 MHz (for ^{1}H NMR) using $CDCl_3$ as a solvent. Differential scanning calorimetry (DSC) was carried out on a TA instruments 2920 Differential Scanning Calorimeter. The heating and cooling rates were 5 °C/min. All polarizing optical microscopy images were recorded with a Leica MPS-30 polarizing optical microscope equipped with a Mettler FP-82HT hot-stage controlled by a Mettler FP-90 central processor. The Fourier transform infrared (FT-IR) measurements were performed on a Bomem MB 100 FT-IR spectrophotometer in combination with a deuterated triglycine sulfate (DTGS) detector. Polymer samples were dissolved in $CHCl_3$ and cast onto a potassium bromide (KBr) window. Before measuring, all the polymers were heated above their isotropic transition temperature and then cooled to 25 °C. X-ray diffraction patterns were recorded on both Kodak Direct Exposure film and a phosphor image plate (Molecular Dynamics®) in a Statton camera using polymer powders. Monochromatic Cu Kα radiation from rotating an anode X-ray generator operating 40 kV and 240 mA was used.

2.3. Synthesis

2.3.1. Preparation of (3-n-octylthio)propanol

To a solution of sodium ethoxide (0.75 g, 11.0 mmol) in 10 ml ethanol was added 1-octanethiol (0.74 g, 5.00 mmol). The mixture was stirred at room temperature for 20 min, and then 3-bromopropanol (0.72 g, 5.00 mmol) was added, and stirred for 1 h. To the reaction mixture, 3 wt% hydrochloride aqueous solution (20 ml) was added, then the aqueous solution was extracted with chloroform. The organic layer was dried over magnesium sulfate. The solvent was removed to give 1.00 g (4.88 mmol) of colorless oil. ^{1}H NMR ($CDCl_3$): δ 0.88 (t, 3H, $J = 6.85$ Hz, $-CH_3$), 1.24–1.37 (m, 10H, $CH_3-(CH_2)_5-CH_2-CH_2-S-$), 1.59 (m, 2H, $CH_3-(CH_2)_5-CH_2-CH_2-S-$), 1.85 (m, 2H, $-S-CH_2-CH_2-CH_2-OH$), 2.47 (t, 2H, $J = 8.24$ Hz, $-CH_2-S-CH_2-CH_2-CH_2-OH$), 2.66 (t, 2H, $J = 6.81$ Hz, $-CH_2-S-CH_2-CH_2-CH_2-OH$), and 3.76 (t, 2H, $J = 6.02$ Hz, $-S-CH_2-CH_2-CH_2-OH$).

2.3.2. Preparation of (3-n-octylsulfonyl)propanol

To a stirred solution of (3-*n*-octylthio)propanol (1.00 g, 4.88 mmol) in chloroform was added *m*-chloroperoxybenzoic acid (*m*-CPBA, 2.96 g, 13.2 mmol) for 1 h at room temperature. The solvent in the mixture was removed and the residue was washed with ether. A 0.95 g (4.03 mmol) of a white solid product was obtained. ^{1}H NMR ($CDCl_3$): δ 0.88 (t, 3H, $J = 7.04$ Hz, $-CH_3$), 1.28–1.44 (m, 10H, CH_3-

(CH_2)$_5$–CH_2–CH_2–SO_2–), 1.85 (m, 2H, CH_3–(CH_2)$_5$–CH_2–CH_2–SO_2–), 2.11 (m, 2H, –SO_2–CH_2–CH_2–CH_2–OH), 3.00 (t, 2H, $J = 5.49$ Hz, –CH_2–SO_2–CH_2–CH_2–CH_2–OH), 3.13 (t, 2H, $J = 7.66$ Hz, –CH_2–SO_2–CH_2–CH_2–CH_2–OH), and 3.82 (t, 2H, $J = 5.86$ Hz, –SO_2–CH_2–CH_2–CH_2–OH).

2.3.3. Preparation of methyl (3-n-octylsulfonyl)propane sulfonate

Into a solution of (3-*n*-octylsulfonyl)propanol (0.95 g, 4.03 mmol) and methanesulfonyl chloride (0.61 g, 5.24 mmol) in CH_2Cl_2 was added triethylamine (0.62 g, 6.05 mmol). The reaction mixture was stirred for 1 h at room temperature, and then was washed two times with 20 ml of hydrochloride 3 wt% aqueous solution. The organic layer was dried over magnesium sulfate. The solvent was removed to give 1.13 g (3.60 mmol) of pale yellow oil, which was used at next step without purification. ^{1}H NMR ($CDCl_3$): δ 0.88 (t, 3H, $J = 7.08$ Hz, –CH_3), 1.27–1.47 (m, 10H, CH_3–(CH_2)$_5$–CH_2–CH_2–SO_2–), 1.85 (m, 2H, CH_3–(CH_2)$_5$–CH_2–CH_2–SO_2–), 2.33 (m, 2H, –SO_2–CH_2–CH_2–CH_2–OSO_2–CH_3), 2.97–3.14 (m, 7H, –CH_2–CH_2–SO_2–CH_2–CH_2–CH_2–OSO_2–CH_3), and 4.41 (t, 2H, $J = 5.86$ Hz, –SO_2–CH_2–CH_2–CH_2–OSO_2–CH_3).

2.3.4. Preparation of (3-n-octylsulfonyl)propyl thioacetate

To a stirred solution of methyl (3-*n*-octylsulfonyl)propane sulfonate (1.13 g, 3.60 mmol) and thioacetic acid (0.51 g, 6.48 mmol) in $CHCl_3$ was added triethylamine (0.52 g, 5.04 mmol). The reaction mixture was refluxed for 3 h. It was washed two times with hydrochloride 3 wt% aqueous solution and 10 wt% aqueous ammonia, respectively. The organic layer was dried over anhydrous magnesium sulfate and the solvent was removed. Chromatography (SiO_2, ethyl acetate/*n*-hexane = 1/2) of the resulting residue afforded 0.69 g (2.35 mmol) of **4**. ^{1}H NMR ($CDCl_3$): δ 0.89 (t, 3H, $J = 6.78$ Hz, –CH_3), 1.28–1.92 (m, 16H, CH_3–(CH_2)$_6$–CH_2–SO_2–CH_2–(CH_2)$_2$–$SCOCH_3$), 2.34 (s, 3H, –SCOCH_3), and 2.88–2.99 (m, 4H, –CH_2–CH_2–SO_2–CH_2–CH_2–).

2.3.5. Preparation of (4-n-octylsulfonyl)butyl thioacetate

This compound was prepared from the same procedure as compound (3-*n*-octylsulfonyl)propyl thioacetate except that 4-bromobutanol was used. ^{1}H NMR ($CDCl_3$): δ 0.88 (t, 3H, $J = 6.96$ Hz, –CH_3), 1.22–1.97 (m, 18H, CH_3–(CH_2)$_6$–CH_2–SO_2–CH_2–(CH_2)$_3$–$SCOCH_3$), 2.34 (s, 3H, –SCOCH_3), and 2.88–2.99 (m, 4H, –CH_2–CH_2–SO_2–CH_2–CH_2–).

2.3.6. Preparation of (5-n-octylsulfonyl)pentyl thioacetate

This compound was prepared from the same procedure as compound (3-*n*-octylsulfonyl)propyl thioacetate except that 5-bromopentanol was used. ^{1}H NMR ($CDCl_3$): δ 0.88 (t, 3H, $J = 6.62$ Hz, –CH_3), 1.28–1.90 (m, 20H, CH_3–(CH_2)$_6$–CH_2–SO_2–CH_2–(CH_2)$_4$–$SCOCH_3$), 2.33 (s, 3H, –SCOCH_3), and 2.84–2.99 (m, 4H, –CH_2–CH_2–SO_2–CH_2–CH_2–).

2.3.7. Preparation of (6-n-octylsulfonyl)hexyl thioacetate

This compound was prepared from the same procedure as compound (3-*n*-octylsulfonyl)propyl thioacetate except that 6-bromohexanol was used. ^{1}H NMR ($CDCl_3$): δ 0.88 (t, 3H, $J = 6.42$ Hz, –CH_3), 1.28–1.84 (m, 22H, CH_3–(CH_2)$_6$–CH_2–SO_2–CH_2–(CH_2)$_5$–$SCOCH_3$), 2.33 (s, 3H, –SCOCH_3), and 2.84–2.97 (m, 4H, –CH_2–CH_2–SO_2–CH_2–CH_2–).

2.3.8. Preparation of (7-n-octylsulfonyl)heptyl thioacetate

This compound was prepared from the same procedure as compound (3-*n*-octylsulfonyl)propyl thioacetate except that 7-bromoheptanol was used. ^{1}H NMR ($CDCl_3$): δ 0.88 (t, 3H, $J = 6.67$ Hz, –CH_3), 1.27–1.89 (m, 24H, CH_3–(CH_2)$_6$–CH_2–SO_2–CH_2–(CH_2)$_6$–$SCOCH_3$), 2.34 (s, 3H, –SCOCH_3), and 2.85–3.00 (m, 4H, –CH_2–CH_2–SO_2–CH_2–CH_2–).

2.3.9. Preparation of (9-n-octylsulfonyl)nonyl thioacetate

This compound was prepared from the same procedure as compound (3-*n*-octylsulfonyl)propyl thioacetate except that 9-bromonanol was used. ^{1}H NMR ($CDCl_3$): δ 0.88 (t, 3H, $J = 6.93$ Hz, –CH_3), 1.28–1.88 (m, 28H, CH_3–(CH_2)$_6$–CH_2–SO_2–CH_2–(CH_2)$_8$–$SCOCH_3$), 2.33 (s, 3H, –SCOCH_3), and 2.84–2.96 (m, 4H, –CH_2–CH_2–SO_2–CH_2–CH_2–).

2.3.10. Preparation of (12-n-octylsulfonyl)dodecyl thioacetate

This compound was prepared from the same procedure as compound (3-*n*-octylsulfonyl)propyl thioacetate except that 12-bromododecanol was used. ^{1}H NMR ($CDCl_3$): δ 0.88 (t, 3H, $J = 6.64$ Hz, –CH_3), 1.21–1.86 (m, 34H, CH_3–(CH_2)$_6$–CH_2–SO_2–CH_2–(CH_2)$_{11}$–$SCOCH_3$), 2.36 (s, 3H, –SCOCH_3), and 2.93–3.10 (m, 4H, –CH_2–CH_2–SO_2–CH_2–CH_2–).

2.3.11. Preparation of ((3-n-octylsulfonyl)propylthio)-methyl-substituted poly(oxyethylene) (OTP-3)

To a stirred solution of sodium ethoxide (0.17 g, 2.49 mmol) in ethanol (10 ml) was added (3-*n*-octylsulfonyl)propyl thioacetate (0.69 g, 2.35 mmol). After stirring at room temperature for 20 min, the reaction mixture was transferred into a solution of poly[oxy(chloromethyl)ethylene] (0.14 g, 1.47 mmol) (PECH) in DMAc (20 ml). The reaction mixture was stirred at 60 °C for 1 h and then poured into distilled water. The precipitate was purified by several precipitations from $CHCl_3$ into methanol and then dried under high vacuum at room temperature overnight. This product was obtained in 93% yield. ^{1}H NMR ($CDCl_3$): δ 0.88 (t, 3H, $J = 6.78$ Hz, –CH_3), 1.20–2.00 (m, 14H, CH_3–(CH_2)$_6$–CH_2–SO_2–CH_2–CH_2–CH_2–S–), 2.56–2.96 (m,

4H, $-CH_2-CH_2-S-CH_2-$), 2.99 (m, 4H, $CH_2-CH_2-SO_2-CH_2-CH_2-$), and 3.60–3.83 (m, 3H, $-O-CH_2-CH-$). ^{13}C NMR ($CDCl_3$): δ 14.5 (s, 1C, $-CH_3$), 22.3 (s, 1C, $-SO_2-CH_2-CH_2-CH_2-CH_2-$), 22.9 (s, 1C, $-CH_2-CH_3$), 28.7–32.0 (m, 5C, $-CH_2-CH_2-SO_2-CH_2-CH_2-(CH_2)_4-CH_2-$), 33.4 (s, 1C, $-S-CH_2-CH_2-CH_2-SO_2-$), 39.1 (s, 1C, $-CH_2-S-CH_2-$), 53.6 (m, 2C, $-CH_2-SO_2-CH_2-$), 70.1–71.3 (m, 1C, $-OCH_2-CH-$), 79.1 (s, 1C, $-O-CH_2-CH-$).

2.3.12. Preparations of ((4-n-octylsulfonyl)butylthio)-methyl-substituted poly(oxyethylene) (OTP-4), ((5-n-octyl-sulfonyl)pentylthio)methyl-substituted poly(oxyethylene) (OTP-5), ((6-n-octylsulfonyl)hexylthio)methyl-substituted poly(oxyethylene) (OTP-6), ((7-n-octylsulfonyl)heptylthio)-methyl-substituted poly(oxyethylene) (OTP-7), ((9-n-octyl-sulfonyl)-nonylthio)methyl-substituted poly(oxyethylene) (OTP-9), and ((12-n-octylsulfonyl)dodecylthio)methyl-substituted poly(oxyethylene) (OTP-12)

All six polymers were synthesized from the same procedure, which was used for the synthesis of OTP-3, except that (4-*n*-octylsulfonyl)butyl thioacetate, (5-*n*-octyl-sulfonyl)pentyl thioacetate, (6-*n*-octylsulfonyl)hexyl thio-acetate, (7-*n*-octylsulfonyl)heptyl thioacetate, (9-*n*-octylsulfonyl)nonyl thioacetate, and (12-*n*-octylsulfonyl)-dodecyl thioacetate were used for OTP-4, OTP-5, OTP-6, OTP-7, OTP-9 and OTP-12, respectively, instead of (3-*n*-octylsulfonyl)propyl thioacetate for OTP-3. NMR results of OTP-4 are as follows. ^1H NMR ($CDCl_3$): $\delta = 0.89$ (t, 3H, $J = 6.79$ Hz, $-CH_3$), 1.20–1.99 (m, 16H, $CH_3-(CH_2)_6-CH_2-SO_2-CH_2-(CH_2)_2-CH_2-S-$), 2.59–2.80 (m, 4H, $-CH_2-CH_2-S-CH_2-$), 3.00 (m, 4H, $CH_2-CH_2-SO_2-CH_2-CH_2-$), 3.57–3.75 (m, 3H, $-O-CH_2-CH-$). ^{13}C NMR ($CDCl_3$): 14.2 (s, 1C, $-CH_3$), 22.1 (s, 1C, $-SO_2-CH_2-CH_2-CH_2-CH_2-$), 22.7 (s, 1C, $-CH_2-CH_3$), 28.3–32.2 (m, 6C, $-(CH_2)_2-CH_2-SO_2-CH_2-CH_2-(CH_2)_4-CH_2-CH_3$), 33.6 (s, 1C, $-S-CH_2-CH_2-CH_2-$), 39.4 (s, 1C, $-CH_2-S-CH_2-$), 53.8 (m, 2C, $-CH_2-SO_2-CH_2-$), 70.2–71.5 (m, 1C, $-OCH_2-CH-$), 79.2 (s, 1C, $-O-CH_2-CH-$). Tables 1 and 2 shows the NMR results of the other polymers.

2.3.13. Preparation of ((3-n-octylsulfonyl)propylsulfonyl)-methyl-substituted poly(oxyethylene) (OSP-3)

To a stirred solution of poly[oxy(((3-*n*-octylsulfonyl)-propylthio)methyl)ethylene] (0.28 g, 0.91 mmol) in chloro-form (10 ml) was added *m*-CPBA (0.45 g, 2.01 mmol). After stirring at room temperature for 1 h, the reaction mixture was concentrated and the residue was dissolved in chloroform (ca. 2 ml). The solution was poured into methanol, and the precipitate was purified by several reprecipitations from chloroform solution into methanol until all *m*-chloroperoxybenzoic acid and *m*-chlorobenzoic acid were removed. The polymer was dried under vacuum at room temperature overnight. The conversion was 100%. ^1H NMR ($CDCl_3$): δ 0.88 (t, 3H, $J = 6.60$ Hz, $-CH_3$), 1.20–1.60 (m, 10H, $-SO_2-CH_2-CH_2-(CH_2)_5-CH_3$), 1.83 (m, 4H, $-SO_2-CH_2-CH_2-CH_2-SO_2-CH_2-CH_2-$), 2.85–3.20 (m, 6H, $-SO_2-CH_2-CH_2-CH_2-SO_2-CH_2-CH_2-$), 3.30 (br s, 2H, $-O-CH_2-CH-CH_2-SO_2-$), 3.55–3.95 (m, 2H, $-O-CH_2-CH-$), and 4.08 (br s, 1H, $-O-CH_2-CH-$). ^{13}C NMR ($CDCl_3$): δ 14.3 (s, 1C, $-CH_3$), 22.1 (s, 1C, $-SO_2-CH_2-CH_2-(CH_2)_5-CH_3$), 22.7 (s, $-CH_2-CH_3$), 28.3–32.1 (m, 5C, $-CH_2-CH_2-SO_2-CH_2-CH_2-(CH_2)_4-CH_2-CH_3$), 52.7 (m, 3C, $-SO_2-CH_2-CH_2-CH_2-SO_2-CH_2-$), 55.2 (s, 1C, $-CH_2-SO_2-(CH_2)_3-SO_2-$), 67.8–70.3 (m, 1C, $-OCH_2-CH-$), 74.2 (s, 1C, $-O-CH_2-CH-$).

2.3.14. Preparations of ((4-n-octylsulfonyl)butylsulfonyl)-methyl-substituted poly(oxyethylene) (OSP-4), ((5-n-octyl-sulfonyl)pentylsulfonyl)methyl-substituted poly-(oxyethylene) (OSP-5), ((6-n-octylsulfonyl)hexylsulfonyl)-methyl-substituted poly(oxyethylene) (OSP-6), ((7-n-octyl-sulfonyl)heptyl-sulfonyl)methyl-substituted poly(oxyethylene) (OSP-7), ((9-n-octyl-sulfonyl)nonyl-sulfonyl)methyl-substituted poly(oxyethylene) (OSP-9), and ((12-n-octylsulfonyl)dodecylsulfonyl)methyl-substituted poly(oxyethylene) (OSP-12)

All six polymers were synthesized from the same procedure, which was used for the synthesis of OSP-3, except that OTP-4, OTP-5, OTP-6, OTP-7, OTP-9 and OTP-12 were used for OSP-4, OSP-5, OSP-6, OSP-7, OSP-9 and OSP-12, respectively, instead of OTP-3 for OSP-3. Tables 1 and 2 shows the NMR results of these polymers.

3. Results and discussion

3.1. Synthesis

Scheme 1 shows the synthesis of ((*n*-octylsulfonyl)-alkylthio)methyl-substituted poly(oxyethylene) (OTP-*M*; $M = 3, 4, 5, 6, 7, 9, 12$) and ((*n*-octylsulfonyl)alkylsulfo-nyl)methyl-substituted poly(oxyethylene) (OSP-*M*; $M = 3, 4, 5, 6, 7, 9, 12$). OTP-M was synthesized by the reaction of PECH and (*n*-octylsulfonyl)alkyl thioacetate (**4**) with sodium ethoxide in DMAc. Sodium ethoxide was prepared by adding sodium into absolute ethanol under a nitrogen atmosphere before use. **4** was prepared by a substitution reaction of methyl (*n*-octylsulfonyl)alkyl thio-acetate (**3**) using thioacetate in $CHCl_3$. **3** was obtained from oxidation of (3-*n*-octylthio)alkanol (**1**) using *m*-CPBA followed by a mesylation reaction. **1** was prepared by a alkylation reaction of bromoalkanol with 1-octanethiol. The degree of conversion from PECH to OTP-M was calculated using ^1H NMR. For example the degree of conversion of OTP-6 was calculated by comparing the integral of the triplet in Fig. 1(a) at 0.89 ppm (a, three protons) with the integral of the backbone peaks at 3.53–3.80 ppm (f, three protons); it was 100% within experimental error. The degrees of conversion of other OTP-Ms were calculated by

Table 1
^{1}H NMR spectral data for the polymers

Polymer	Chemical shifts[a] (δ, ppm)
OTP-5	0.89 (t, 3H, $J = 6.60$, $-CH_3$), 1.28–1.85 (m, 18H, $CH_3-(CH_2)_6-CH_2-SO_2-CH_2-(CH_2)_3-CH_2-S-$), 2.56–2.76 (m, 4H, $-CH_2-CH_2-S-CH_2-$), 2.96 (m, 4H, $CH_2-CH_2-SO_2-CH_2-CH_2-$), 3.59–3.71 (m, 3H, $-O-CH_2-CH-$)
OTP-6	0.89 (t, 3H, $J = 6.90$, $-CH_3$), 1.29–1.83 (m, 20H, $CH_3-(CH_2)_6-CH_2-SO_2-CH_2-(CH_2)_4-CH_2-S-$), 2.48–2.70 (m, 4H, $-CH_2-CH_2-S-CH_2-$), 2.95 (m, 4H, $CH_2-CH_2-SO_2-CH_2-CH_2-$), 3.53–3.80 (m, 3H, $-O-CH_2-CH-$)
OTP-7	0.88 (t, 3H, $J = 6.78$, $-CH_3$), 1.22–1.85 (m, 22H, $CH_3-(CH_2)_6-CH_2-SO_2-CH_2-(CH_2)_5-CH_2-S-$), 2.52–2.73 (m, 4H, $-CH_2-CH_2-S-CH_2-$), 2.94 (m, 4H, $CH_2-CH_2-SO_2-CH_2-CH_2-$), 3.48–3.63 (m, 3H, $-O-CH_2-CH-$)
OTP-9	0.88 (t, 3H, $J = 6.90$, $-CH_3$) 1.31–1.88 (m, 26H, $CH_3-(CH_2)_6-CH_2-SO_2-CH_2-(CH_2)_7-CH_2-S-$), 2.52–2.70 (m, 4H, $-CH_2-CH_2-S-CH_2-$), 2.94 (m, 4H, $CH_2-CH_2-SO_2-CH_2-CH_2-$), 3.50–3.78 (m, 3H, $-O-CH_2-CH-$)
OTP-12	0.89 (t, 3H, $J = 6.79$, $-CH_3$), 1.23–1.88 (m, 32H, $CH_3-(CH_2)_6-CH_2-SO_2-CH_2-(CH_2)_{10}-CH_2-S-$), 2.48–2.68 (m, 4H, $-CH_2-CH_2-S-CH_2-$), 2.94 (m, 4H, $CH_2-CH_2-SO_2-CH_2-CH_2-$), 3.50–3.78 (m, 3H, $-O-CH_2-CH-$)
OSP-4	0.89 (t, 3H, $J = 6.70$, $-CH_3$), 1.20–1.58 (m, 10H, $-CH_2-SO_2-CH_2-CH_2-(CH_2)_5-CH_3$), 1.88 (m, 6H, $-SO_2-CH_2-(CH_2)_2-CH_2-SO_2-CH_2-CH_2-$), 2.98–3.07 (m, 6H, $-SO_2-CH_2-(CH_2)_2-CH_2-SO_2-CH_2-CH_2-$), 3.15 (br s, 2H, $-O-CH_2-CH-CH_2-SO_2-$), 3.65–3.74 (m, 2H, $-O-CH_2-CH-$), 4.12 (br s, 1H, $-O-CH_2-CH-$)
OSP-5	0.89 (t, 3H, $J = 6.90$, $-CH_3$) 1.29–1.59 (m, 12H, $-CH_2-CH_2-CH_2-SO_2-CH_2-CH_2-(CH_2)_5-CH_3$), 1.87 (m, 6H, $-SO_2-CH_2-CH_2-CH_2-CH_2-CH_2-SO_2-CH_2-CH_2-$), 3.00–3.09 (m, 6H, $-SO_2-CH_2-(CH_2)_3-CH_2-SO_2-CH_2-CH_2-$), 3.37 (br s, 2H, $-O-CH_2-CH-CH_2-SO_2-$), 3.70–3.83 (m, 2H, $-O-CH_2-CH-$), 4.12 (br s, 1H, $-O-CH_2-CH-$)
OSP-6	0.89 (t, 3H, $J = 6.88$, $-CH_3$), 1.30–1.56 (m, 14H, $-(CH_2)_2-CH_2-CH_2-SO_2-CH_2-CH_2-(CH_2)_5-CH_3$), 1.84 (m, 6H, $-SO_2-CH_2-CH_2-(CH_2)_2-CH_2-CH_2-SO_2-CH_2-CH_2-$), 2.98–3.10 (m, 6H, $-SO_2-CH_2-(CH_2)_4-CH_2-SO_2-CH_2-CH_2-$), 3.28 (br s, 2H, $-O-CH_2-CH-CH_2-SO_2-$), 3.69–3.80 (m, 2H, $-O-CH_2-CH-$), 4.11 (br s, 1H, $-O-CH_2-CH-$)
OSP-7	0.89 (t, 3H, $J = 6.60$, $-CH_3$), 1.22–1.57 (m, 16H, $-(CH_2)_3-CH_2-CH_2-SO_2-CH_2-CH_2-(CH_2)_5-CH_3$), 1.81 (m, 6H, $-SO_2-CH_2-CH_2-(CH_2)_3-CH_2-CH_2-SO_2-CH_2-CH_2-$), 2.96–2.98 (m, 6H, $-SO_2-CH_2-(CH_2)_5-CH_2-SO_2-CH_2-CH_2-$), 3.29 (br s, 2H, $-O-CH_2-CH-CH_2-SO_2-$), 3.66–3.80 (m, 2H, $-O-CH_2-CH-$), 4.07 (br s, 1H, $-O-CH_2-CH-$)
OSP-9	0.88 (t, 3H, $J = 7.20$, $-CH_3$), 1.19–1.63 (m, 20H, $-(CH_2)_5-CH_2-CH_2-SO_2-CH_2-CH_2-(CH_2)_5-CH_3$), 1.83 (m, 6H, $-SO_2-CH_2-CH_2-(CH_2)_5-CH_2-CH_2-SO_2-CH_2-CH_2-$), 2.91–2.97 (m, 6H, $-SO_2-CH_2-(CH_2)_7-CH_2-SO_2-CH_2-CH_2-$), 3.28 (br s, 2H, $-O-CH_2-CH-$), 3.63–3.72 (m, 2H, $-O-CH_2-CH-$), 4.11 (br s, 1H, $-O-CH_2-CH-$)
OSP-12	0.88 (t, 3H, $J = 7.10$, $-CH_3$), 1.27–1.56 (m, 26H, $-(CH_2)_8-CH_2-CH_2-SO_2-CH_2-CH_2-(CH_2)_5-CH_3$), 1.83 (m, 6H, $-SO_2-CH_2-CH_2-(CH_2)_8-CH_2-CH_2-SO_2-CH_2-CH_2-$), 2.91–2.96 (m, 6H, $-SO_2-CH_2-(CH_2)_{10}-CH_2-SO_2-CH_2-CH_2-$), 3.26 (br s, 2H, $-O-CH_2-CH-$), 3.62–3.71 (m, 2H, $-O-CH_2-CH-$), 4.11 (br s, 1H, $-O-CH_2-CH-$)

[a] In $CDCl_3$.

similar manners and they are listed in Table 3. For all the other OTP-Ms, conversions were found to be higher than 90%. Although the degree of conversion of PECH to OTP-Ms was not always 100%, it would not affect the conclusions of this paper. Because most properties including thermal and morphological properties of polymers including liquid crystalline polymers with 100 and 90% side group substitutions are very close [18–21]. OSP-Ms were obtained by the oxidation of corresponding OTP-Ms using *m*-CPBA. The structures of the products were confirmed by the ^{1}H NMR spectra of the polymers. For example, Fig. 1(b) shows a ^{1}H NMR spectrum of OSP-6. The degree of conversion from OTP-M to corresponding OSP-M was always 100% (Table 3).

Molecular weights and polydispersity indexes obtained by GPC using polystyrene standards are listed in Table 3. The number-average molecular weights of the OTP-Ms and OSP-Ms range from about 15,000 to 167,000. Although the molecular weights of some polymers are not very high, still these values are high enough to ignore the effect of the molecular weights on the thermal transition temperatures of the polymers [22,23].

3.2. Thermal behavior

Fig. 2 shows normalized DSC curves of OTP-Ms and OSP-Ms obtained during second heating scans at a rate of 5 °C/min. Multiple endotherms and exotherms from the heating and cooing scans, respectively, were observed for all cases. The transition temperatures and the enthalpy changes of the endotherms are listed in Table 4 (very small peaks are not listed). Previous results on similar polymers such as ((*n*-alkylsulfonyl)hexylthio)methyl-substituted poly(oxyethylene)s and ((*n*-alkylsulfonyl)alkylsulfonyl)-methyl-substituted poly(oxyethylene)s indicate that the endotherms obtained from the DSC heating scans are due to the phase transitions from smectic B to smectic A phases, from highly ordered smectic B to less ordered smectic B phases, and/or from smectic A to isotropic phases, which were decided by X-ray experiments [10,11]. The detailed studies on structural changes of the OTP-Ms and OSP-Ms with varied temperatures are under progress to elucidate the structural changes. However, some of the X-ray results and phase transition behavior at around isotropic temperatures from POM studies are shown in the next paragraph.

For all OTP-Ms and OSP-3 spherulites were observed when the samples were cooled down from isotropic melt states. For example, when OTP-9 was cooled from the isotropic melt state, very small points started to appear from the isotropic melt from about 90 °C and within a few minutes they turned into typical spherulites and then

Table 2
^{13}C NMR spectral data for the polymers

Polymer	Chemical shifts[a] (δ, ppm)
OTP-5	14.4 (s, 1C, $-CH_3$), 22.5 (s, 1C, $-SO_2-CH_2-CH_2-CH_2-CH_2-$), 22.8 (s, 1C, $-CH_2-CH_3$), 28.4–32.5 (m, 7C, $-(CH_2)_3-CH_2-SO_2-CH_2-CH_2-(CH_2)_4-CH_2-CH_3$), 33.8 (s, 1C, $-S-CH_2-CH_2-CH_2-$), 39.2 (s, 1C, $-CH_2-S-CH_2-$), 53.2 (m, 2C, $-CH_2-SO_2-CH_2-$), 70.0–71.3 (m, 1C, $-OCH_2-CH-$), 79.1 (s, 1C, $-O-CH_2-CH-$)
OTP-6	14.3 (s, 1C, $-CH_3$), 22.4 (s, 1C, $-SO_2-CH_2-CH_2-CH_2-CH_2-$), 22.6 (s, 1C, $-CH_2-CH_3$), 28.2–32.9 (m, 8C, $-(CH_2)_4-CH_2-SO_2-CH_2-CH_2-(CH_2)_4-CH_2-CH_3$), 34.1 (s, 1C, $-S-CH_2-CH_2-CH_2-$), 39.5 (s, 1C, $-CH_2-S-CH_2-$), 53.1 (m, 2C, $-CH_2-SO_2-CH_2-$), 70.3–71.4 (m, 1C, $-OCH_2-CH-$), 79.3 (s, 1C, $-O-CH_2-CH-$)
OTP-7	14.2 (s, 1C, $-CH_3$), 22.3 (s, 1C, $-SO_2-CH_2-CH_2-CH_2-CH_2-$), 22.9 (s, 1C, $-CH_2-CH_3$), 28.5–32.6 (m, 9C, $-(CH_2)_5-CH_2-SO_2-CH_2-CH_2-(CH_2)_4-CH_2-CH_3$), 33.6 (s, 1C, $-S-CH_2-CH_2-CH_2-$), 39.5 (s, 1C, $-CH_2-S-CH_2-$), 53.0 (m, 2C, $-CH_2-SO_2-CH_2-$), 70.2–71.3 (m, 1C, $-OCH_2-CH-$), 79.2 (s, 1C, $-O-CH_2-CH-$)
OTP-9	14.4 (s, 1C, $-CH_3$), 22.6 (s, 1C, $-SO_2-CH_2-CH_2-CH_2-CH_2-$), 23.1 (s, 1C, $-CH_2-CH_3$), 28.7–33.1 (m, 11C, $-(CH_2)_7-CH_2-SO_2-CH_2-CH_2-(CH_2)_4-CH_2-CH_3$), 33.9 (s, 1C, $-S-CH_2-CH_2-CH_2-$), 39.7 (s, 1C, $-CH_2-S-CH_2-$), 53.3 (m, 2C, $-CH_2-SO_2-CH_2-$), 70.0–71.4 (m, 1C, $-OCH_2-CH-$), 79.1 (s, 1C, $-O-CH_2-CH-$)
OTP-12	14.4 (s, 1C, $-CH_3$), 22.3 (s, 1C, $-SO_2-CH_2-CH_2-CH_2-CH_2-$), 23.0 (s, 1C, $-CH_2-CH_3$), 28.9–32.1 (m, 13C, $-(CH_2)_{10}-CH_2-SO_2-CH_2-CH_2-(CH_2)_4-CH_2-CH_3$), 33.6 (s, 1C, $-S-CH_2-CH_2-CH_2-$), 39.6 (s, 1C, $-CH_2-S-CH_2-$), 53.1 (m, 2C, $-CH_2-SO_2-CH_2-$), 70.2–71.3 (m, 1C, $-OCH_2-CH-$), 79.3 (s, 1C, $-O-CH_2-CH-$)
OSP-4	14.3 (s, 1C, $-CH_3$), 22.3 (s, 1C, $-SO_2-CH_2-CH_2-(CH_2)_5-CH_3$), 22.5 (s, $-CH_2-CH_3$), 28.1–32.3 (m, 6C, $-(CH_2)_2-CH_2-SO_2-CH_2-CH_2-(CH_2)_4-CH_2-CH_3$), 52.9 (m, 3C, $-SO_2-CH_2-CH_2-CH_2-SO_2-CH_2-$), 56.1 (s, 1C, $-CH_2-SO_2-(CH_2)_3-SO_2-$), 67.5–70.6 (m, 1C, $-OCH_2CH-$), 76.0 (s, 1C, $-OCH_2CH-$)
OSP-5	14.4 (s, 1C, $-CH_3$), 22.5 (s, 1C, $-SO_2-CH_2-CH_2-(CH_2)_5-CH_3$), 22.9 (s, $-CH_2-CH_3$), 28.6–32.6 (m, 7C, $-(CH_2)_3-CH_2-SO_2-CH_2-CH_2-(CH_2)_4-CH_2-CH_3$), 53.1 (m, 3C, $-SO_2-CH_2-CH_2-CH_2-SO_2-CH_2-$), 55.3 (s, 1C, $-CH_2-SO_2-(CH_2)_3-SO_2-$),67.3–70.4 (m, 1C, $-OCH_2CH-$), 75.9 (s, 1C, $-OCH_2CH-$)
OSP-6	14.4 (s, 1C, $-CH_3$), 21.9 (s, 1C, $-SO_2-CH_2-CH_2-(CH_2)_5-CH_3$), 22.3 (s, $-CH_2-CH_3$), 28.3–32.1 (m, 8C, $-(CH_2)_4-CH_2-SO_2-CH_2-CH_2-(CH_2)_4-CH_2-CH_3$), 52.7 (m, 3C, $-SO_2-CH_2-CH_2-CH_2-SO_2-CH_2-$), 55.0 (s, 1C, $-CH_2-SO_2-(CH_2)_3-SO_2-$), 67.9–70.4 (m, 1C, $-OCH_2CH-$), 75.5 (s, 1C, $-OCH_2CH-$), 67.2–70.1 (m, 1C, $-OCH_2CH-$), 75.7 (s, 1C, $-OCH_2CH-$)
OSP-7	14.5 (s, 1C, $-CH_3$), 22.1 (s, 1C, $-SO_2-CH_2-CH_2-(CH_2)_5-CH_3$), 22.9 (s, $-CH_2-CH_3$), 28.6–32.1 (m, 9C, $-(CH_2)_5-CH_2-SO_2-CH_2-CH_2-(CH_2)_4-CH_2-CH_3$), 52.8 (m, 3C, $-SO_2-CH_2-CH_2-CH_2-SO_2-CH_2-$), 55.2 (s, 1C, $-CH_2-SO_2-(CH_2)_3-SO_2-$) 67.8–70.3 (m, 1C, $-OCH_2CH-$), 75.2 (s, 1C, $-OCH_2CH-$)
OSP-9	14.3 (s, 1C, $-CH_3$), 21.6 (s, 1C, $-SO_2-CH_2-CH_2-(CH_2)_5-CH_3$), 22.6. (s, $-CH_2-CH_3$), 28.6–32.3 (m, 11C, $-(CH_2)_7-CH_2-SO_2-CH_2-CH_2-(CH_2)_4-CH_2-CH_3$), 52.9 (m, 3C, $-SO_2-CH_2-CH_2-CH_2-SO_2-CH_2-$), 55.4 (s, 1C, $-CH_2-SO_2-(CH_2)_3-SO_2-$), 67.8–70.9 (m, 1C, $-OCH_2CH-$), 75.0 (s, 1C, $-OCH_2CH-$)
OSP-12	14.5 (s, 1C, $-CH_3$), 22.3 (s, 1C, $-SO_2-CH_2-CH_2-(CH_2)_5-CH_3$), 22.8 (s, $-CH_2-CH_3$), 27.8–32.5 (m, 14C, $-(CH_2)_{10}-CH_2-SO_2-CH_2-CH_2-(CH_2)_4-CH_2-CH_3$), 52.4 (m, 3C, $-SO_2-CH_2-CH_2-CH_2-SO_2-CH_2-$), 55.3 (s, 1C, $-CH_2-SO_2-(CH_2)_3-SO_2-$), 67.4–70.7 (m, 1C, $-OCH_2CH-$), 75.5 (s, 1C, $-OCH_2CH-$)

[a] In $CDCl_3$.

impinged on each other. The spherulites disappeared at 113 °C (isotropic temperature T_i) when the polymer was reheated. Other OTP-Ms and OSP-3 showed the similar behavior at around their T_i's. The spherulitic textures of OTP-6 and OTP-9 are shown in Fig. 3(a) and (b), respectively. Since the backbone of the starting polymer is nonstereoregular, the spherulites of the polymers should arise from the organization of (*n*-octylsulfonyl)alkyl side groups. Therefore, we defined OTP-Ms and OSP-3 as 'side chain crystalline' polymers. IR results, which are given in the *structure* part of this paper, show that the side chains of the polymers have hexagonal packings, indicating that they are not typical crystalline. According to different definitions by others these polymers can also be defined as liquid crystalline [24] or condis crystalline [25]. We just defined OTP-Ms and OSP-3 as side chain crystalline for just convenience to distinguish OTP-Ms and OSP-3 with other OSP-Ms. OSP-Ms with $M \geq 4$ showed typical liquid crystalline textures such as schlieren and focal-conic textures. For example, OSP-5 showed a focal-conic fan texture at 210 °C when the polymer was cooled from the isotropic melt at a cooling rate of 10 °C/min. Further decrease in the temperature did not lead to any significant POM texture change. Only minor birefringence changes were observed. Upon heating the focal-conic fan texture disappeared at around 210 °C. For the other OSP-Ms with $M = 4, 6, 7, 9$ and 12 focal-conic fan textures or schlieren textures were observed from the same experiments while at different temperatures. Their liquid crystalline textures and T_i's are listed in Table 4. Fig. 3(c) and (d) show the liquid crystalline textures of OSP-5 and OSP-6, respectively. These results indicate that OSP-Ms with $M \geq 4$ have liquid crystalline phases. Although we have not finished all the X-ray experiments with various temperature yet, preliminary X-ray results also show that OTP-Ms and OSP-3 are crystalline and OSP-Ms with $M \geq 4$ are liquid crystalline below T_i. OTP-Ms and OSP-3 have sharp wide-angle peaks due to the side chain crystals below their T_i's. OSP-Ms with $M = 4, 6, 7, 9$ and 12 have a broad amorphous halo in the wide angle region and sharp small angle peaks indicating that the polymers are liquid crystalline.

The T_i's (measured with POM) of the side chain

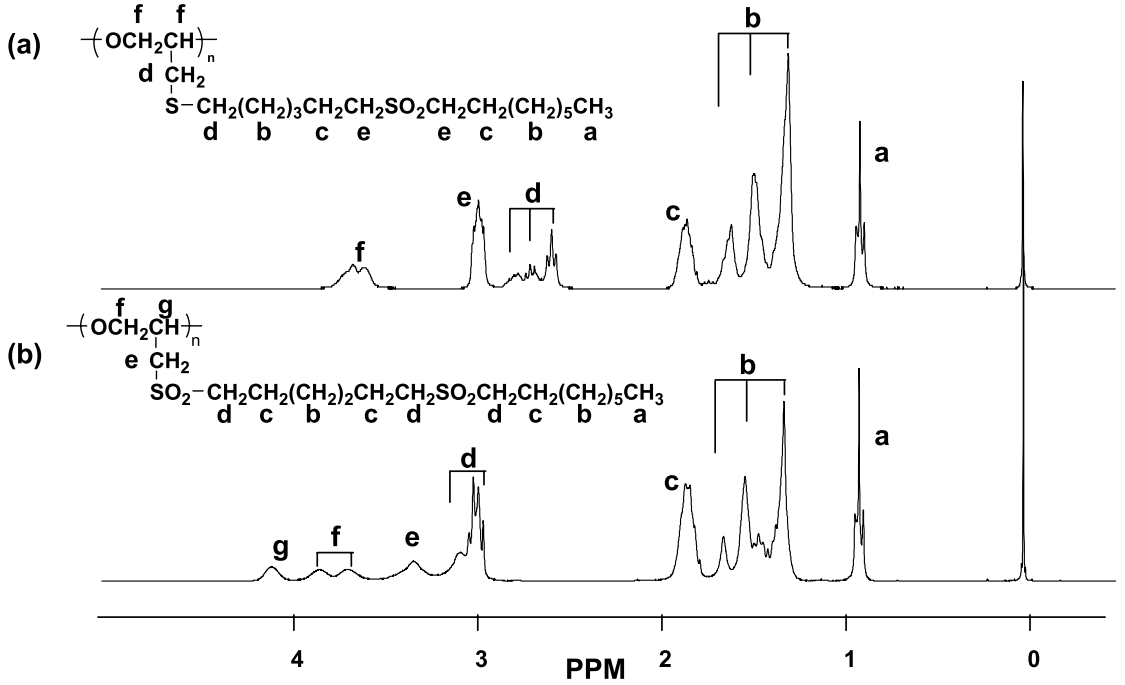

Fig. 1. NMR spectra of (a) OTP-6 and (b) OSP-6.

crystalline polymers (OTP-Ms and OSP-3) are almost identical with the highest transition temperatures (obtained from the heating scans of DSC) for OTP-3, 4, 5 and 9 and with the second highest DSC transition temperature for OTP-6, 7 and 12. For OTP-6, 7 and 12 the values of the enthalpy changes (the size of the peaks) for the second highest DSC transitions were much larger than those for the highest DSC transitions. Although OTP-6, 7 and 12 were annealed for several hours or even several days at a temperature between the highest transition temperatures and the second highest transition temperatures, no birefringent texture was observed from POM. Therefore, the origin of the highest transition temperatures for OTP-6, 7 and 12 is not clear at this time. For the liquid crystalline polymers (OSP-Ms with $M \geq 4$), the T_i's are always higher than the highest transition temperatures obtained from the second heating scans of DSC. However, from the DSC heating scans obtained after annealing these liquid crystalline

Table 3
Conversions and molecular weights for the polymers

Polymer	Conversions (%)		M_n[a]	M_n/M_w
	PECH to OTP-M	OTP-M to OSP-M		
OTP-3	~97		38,300	1.55
OTP-4	~96		20,500	2.68
OTP-5	~100		33,000	3.21
OTP-6	~100		167,100	3.83
OTP-7	~98		139,500	2.35
OTP-9	~100		77,000	1.68
OTP-12	~90		62,300	1.45
OSP-3		~100	29,000	2.76
OSP-4		~100	59,400	1.88
OSP-5		~100	21,200	1.57
OSP-6		~100	40,900	1.36
OSP-7		~100	66,700	1.76
OSP-9		~100	14,900	1.25
OSP-12		~100	15,100	1.28

[a] Obtained from GPC at 35 °C using THF as solvent with monodisperse polystyrenes as standards.

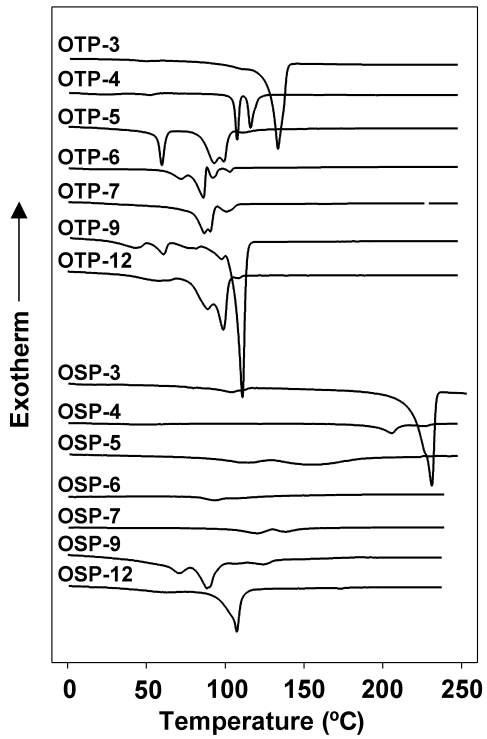

Fig. 2. Normalized DSC second heating curves of OTP-M and OSP-M.

Table 4
DSC and polarizing optical microscopic results for the polymers

Polymer	Second heating endotherms, °C (ΔH, J/g)	First cooling exotherm, °C (ΔH, J/g)	T_i[a] (°C)	Texture[b]
OTP-3	133.4 (81.2)	118.0 (80.1)	135	Spherulite
OTP-4	22.6 (5.0), 51.8 (2.0), 107.5 (24.5), 116.1 (25.1)	110.5 (22.2), 101.7 (19.9)	115	Spherulite
OTP-5	59.8 (19.0), 93.0 (31.4), 96.7 (12.7), 112.2 (1.3)	92.8 (27.9), 71.3 (20.4), 37.2 (18.9)	113	Spherulite
OTP-6	71.6 (31.4), 86.2 (45.3), 92.0 (11.4), 103.1 (2.8)	71.1 (60.8), 60.9 (25.4)	90	Spherulite
OTP-7	86.6 (32.7), 90.5 (15.2), 101.4 (6.8)	75.3 (8.5), 70.6 (54.7)	93	Spherulite
OTP-9	42.7 (6.1), 60.9 (6.3), 76.9 (2.6), 97.5 (2.1), 110.9 (72.9)	91.6 (95.6), 70.8 (0.5), 47.9 (5.4), 37.2 (3.2)	113	Spherulite
OTP-12	57.0 (7.5), 88.3 (34.6), 98.7 (36.3), 108.8 (0.5)	83.6 (72.0), 60.7 (23.4)	99	Spherulite
OSP-3	104.3 (3.8), 231.1 (75.8)	222.3 (75.0), 85.3 (2.6)	230	Spherulite
OSP-4	47.2 (7.5), 121.7 (0.3), 205.9 (37.3), 227.3 (7.1)	222.9 (5.9), 179.4 (30.3), 42.7 (7.5)	255	Focal-conic
OSP-5	99.7 (11.8), 153.0 (32.8)	152.4 (2.7), 114.8 (12.5)	220	Focal-conic
OSP-6	94.2 (15.6), 109.2 (12.5)	100.6 (13.8), 82.6 (11.8)	137	Schlieren
OSP-7	119.6 (22.0), 138.3 (9.3)	117.3 (45.8)	145	Schlieren
OSP-9	70.7 (11.4), 88.3 (24.8), 124.7 (2.7)	94.5 (3.4), 76.1 (26.5), 53.9 (0.9), 43.9 (2.5)	244	Schlieren
OSP-12	58.8 (4.7), 107.4 (46.7)	94.6 (41.4), 62.8 (5.2)	111	Focal-conic

[a] Obtained from heating at 10 °C/min using POM.
[b] Obtained from cooling the isotropic melt at just below the T_i by POM.

polymers at the T_i's (measured with POM) for 1 h, small endotherms were observed at around POM T_i's.

We believe that the major driving force for the formation of liquid crystalline phases of OSP-Ms with $M \geq 4$ is the strong dipole–dipole interactions between the sulfone groups near to the oxyethylene backbone, which in turn can generate a hydrophilic and/or very polar backbone part. Then a phase separation between the hydrophilic (and/or polar) backbone part composed of sulfonylmethyl-substituted oxyethylene units and the hydrophobic (and/or less polar) side tail part composed of (*n*-octylsulfonyl)alkyl side groups can possibly be induce and the liquid crystalline phase can be developed. Akiyama et al. also reported liquid crystalline phase formation of polymers due to a phase separation, where their liquid crystalline polymers are composed of hydrophilic oxymethyl-substituted oxyethylene backbones and hydrophobic alkoxyphenyl side groups [26]. OTP-Ms containing less polar and/or less hydrophilic thiomethyl-substituted oxyethylene backbone units do not have liquid crystalline phases probably because the phase separation between the backbone and side tail parts is not enough. OSP-3 containing (*n*-octylsulfonyl)propyl side groups does not show any typical liquid crystalline behavior, although the chemical structure of OSP-3 is more or less close to other OSP-Ms than OTP-Ms. There is no clear explanation why OSP-3 and OSP-4 show so different thermal and morphological behavior although their structural difference is so minor. One of the possible

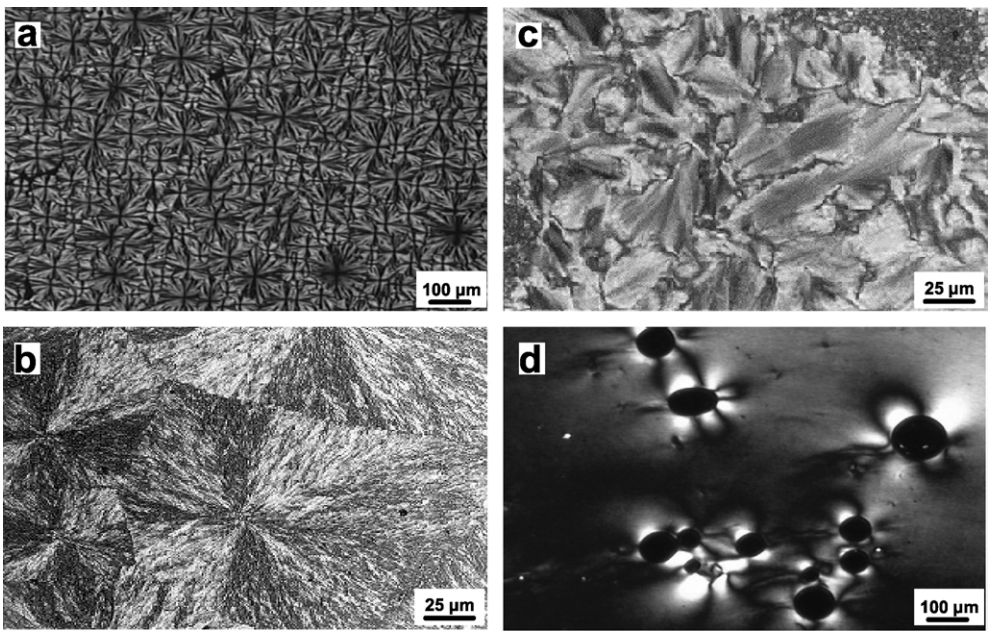

Fig. 3. Cross-polarizing optical microscopic photographs for (a) OTP-6, (b) OTP-9, (c) OSP-5, and (d) OSP-6.

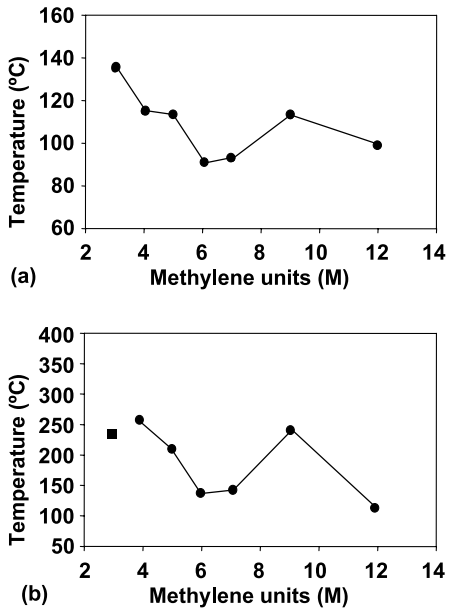

Fig. 4. Plots of isotropic temperature versus the number of methylene groups between the two sulfur atoms (M) of (a) OTP-M, (b) OSP-M.

explanations is that the alkylene group between the two sulfone groups acts as a spacer between the polar backbone part and less polar side chain part, then the propylene group in OSP-3 is not long enough to induce a biphasic structure in the polymer.

It has been reported that T_i's (or T_m's) of flexible or semiflexible backbone polymers with alkyl side chains increase as the side-chain length increases when the alkyl chains form side chain crystalline phases [27,28], while T_i's of rigid backbone polymers decrease with increasing the side-chain length because the alkyl side chains act very similar to solvent by diluting the interactions between the

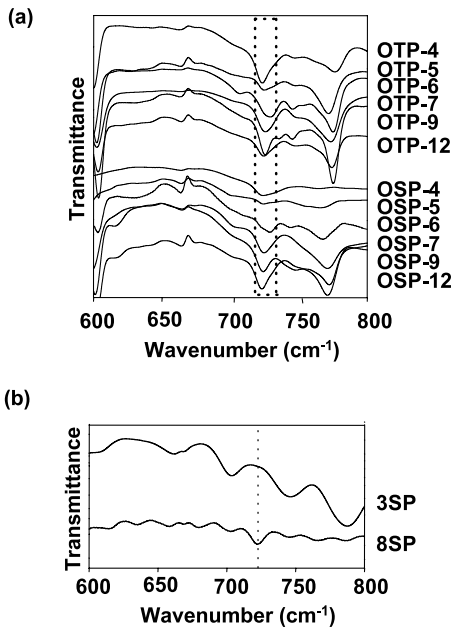

Fig. 5. IR spectra of (a) OTP-Ms and OSP-Ms, and (b) 3SP and 8SP.

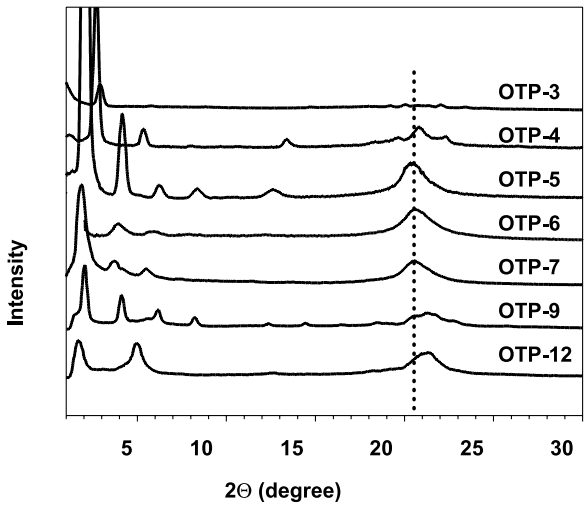

Fig. 6. 2Θ Scans of the X-ray patterns of OTP-M.

rigid polymer backbones [29–32]. However, there is no such discernable trend for the T_i versus M curves of OTP-Ms and OSP-Ms as shown in Fig. 4. This result indicates that the role of the alkylsulfonyl side groups in OTP-Ms and OSP-Ms are different from the alkyl groups in the other polymers. Irregular T_i vs side-chain length curves have been found for liquid crystalline poly(acrylate)s with fluoroalkyl side groups; T_i's of the liquid crystalline poly(acrylate)s with fluoroalkyl side groups decreases with increasing the side chain length, then start to increase beyond a certain length of the side chain [33]. This result has been ascribed to the different layer structures such as double-layer and single-layer structures for the poly(acrylate)s with shorter and longer fluoroalkyl side chains, respectively. We also found that there are two different layer structures for our polymers. This will be discussed in the next part of this paper.

3.3. Structure

Comb-like polymers with hexagonal side chain packings have been characterized by a single IR absorption maximum at around 720 cm^{-1} [10,34,35]. IR spectra of OTP-Ms and OSP-Ms (Fig. 5(a)) also show an absorption maximum at around 720 cm^{-1}. To make sure that those peaks of OTP-Ms and OSP-Ms are not from any other signals in a finger print region, we ran IR experiments of other poly(oxyethylene) derivatives with similar chemical structures such as (*n*-propylsulfonyl)methyl-substituted poly(oxyethylene) (3SP) and (*n*-octylsulfonyl)methyl-substituted poly(oxyethylene) (8SP); 3SP is amorphous and 8SP has a side chain ordered structure [18,36]. In Fig. 5(b), 8SP shows a peak at around 720 cm^{-1}, while 3SP does not. Therefore, we believe that OTP-Ms and OSP-Ms have hexagonal side-chain packings at room temperature.

Comb-like polymers with hexagonal side-chain packings have been also characterized by a wide-angle X-ray *d*-spacing of around 4.20 Å [10,34,35]. Figs. 6 and 7 show the

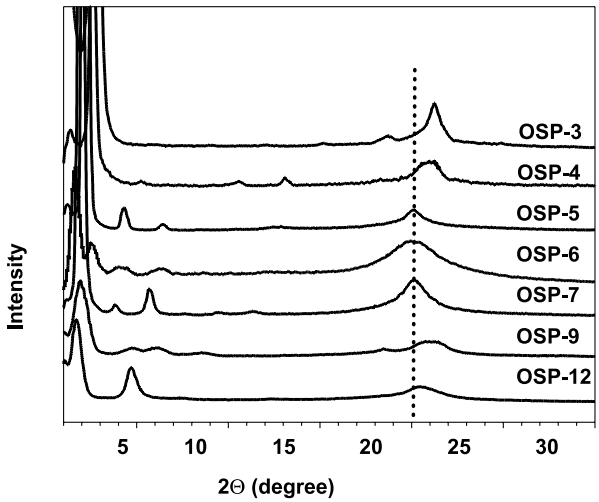

Fig. 7. 2Θ Scans of the X-ray patterns of OSP-M.

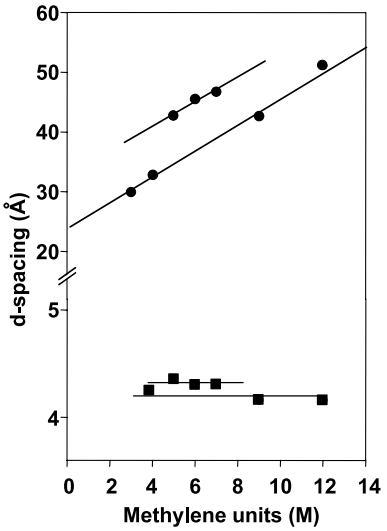

Fig. 8. Plots of wide-angle *d*-spacings (■) inter layer spacings (●) versus the number of methylene groups between the two sulfur atoms (M) of OTP-M.

X-ray powder patterns at room temperature for OTP-Ms and OSP-Ms. The wide-angle *d*-spacings of the polymers are around 4.16–4.43. The *d*-spacings of the most intensive wide-angle peak for OTP-Ms and OSP-Ms with $M = 3, 4, 9$ and 12 are around 4.20 Å, however, those of the polymers with $M = 5, 6, 7$ are larger than 4.20 Å. OTP-5, 6 and 7 have the *d*-spacings of 4.31–4.36Å, and OSP-5, 6 and 7 have the *d*-spacings of 4.41–4.44 Å. These wide-angle peaks for the polymers with $M = 5, 6, 7$ are all broad single peaks, while those of the polymers with $M = 3, 4, 9, 12$ are generally sharper or multiple. These results indicate that the hexagonal side-chain packings of the polymers with $M = 5, 6, 7$ are somewhat different from those of the polymers with $M = 3, 4, 9, 12$.

X-ray data in the smaller angle region confirm that the polymers with $M = 3, 4, 9, 12$ have the different packing structures compared with those of polymers with $M = 5, 6, 7$. Figs. 6 and 7 show a series of ordered reflections in the smaller angle region. The small-angle reflections for the polymers can be assigned to the (001) and (002) planes for lamellar phases; for some polymers even (003), (004), and/or (005) planes were observed. The *d*-spacings of the polymers are calculated using the Bragg equation and they are listed in Table 5. The side-chain lengths (L_{cal}) calculated using atomic bond lengths and angles assuming all anti conformation are listed also; the optimized bond lengths and angles for the calculation were obtained using CS Chem3D Pro® software. The small-angle *d*-spacings of the polymers with $M = 5, 6, 7$ are about twice the corresponding L_{cal} within experimental error. However, the small-angle *d*-spacings of the polymers with $M = 3, 4, 9, 12$ are smaller than the corresponding $2 \times L_{cal}$ by 5.2–10.2 Å. Therefore, it is quite reasonable to assume that the polymers with $M = 5, 6, 7$ have double-layer structures. The polymers with $M = 3, 4, 9, 12$ can have intercalating double-layer structures or tilted side chains about a certain degree from the normal of the backbone. Two-dimensional fiber X-ray patterns of all other similar poly(oxyethylene)s having ordered phases, such as (*n*-octylsulfonyl)methyl-substituted, (*n*-hexadecylsulfony)methyl-substituted, (*n*-hexadecylthio)methyl-substituted, [(*n*-nonylsulfonylhexyl)sulfonyl]methyl-substituted, and [(6-*n*-nonylsulfonyl)hexylthio]methyl-substituted poly(oxyethylene)s showed a series of sharp reflections along the equator and broad outer rings in the wide-angle region having increased intensities on the meridian [10,11,18]. The same two-dimensional fiber X-ray patterns were obtained for OTP-6, OSP-6, and OSP-12. We could not get two-dimensional fiber X-ray patterns of other OTP-Ms and OSP-Ms because we could not make good fibers from them until now. Other X-ray results of comb-like vinyl polymers with alkyl side chains

Table 5
The *d*-spacings determined from the most intensive peak in the wide-angle region and from the first reflection in the small-angle region, and the calculated side chain length (L_{cal})

	Wide-angle (Å)	Small-angle (Å)	$2 \times L_{cal}$[a] (Å)
OTP-3		29.9	37.9
OTP-4	4.26	32.8	40.4
OTP-5	4.36	42.7	42.9
OTP-6	4.31	45.3	45.4
OTP-7	4.31	46.7	47.9
OTP-9	4.16	42.7	52.9
OTP-12	4.16	51.1	60.4
OSP-3	4.18	29.1	36.7
OSP-4	4.18	34.0	39.2
OSP-5	4.41	40.9	41.7
OSP-6	4.44	44.7	44.2
OSP-7	4.43	45.1	46.7
OSP-9	4.17	45.1	51.7
OSP-12	4.23	51.4	59.2

[a] L_{cal} is the calculated length of the side chain using CS Chem3D Pro® software.

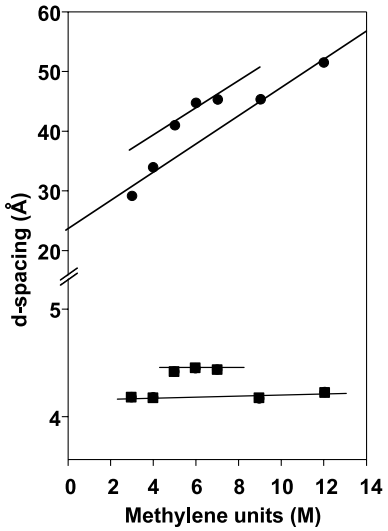

Fig. 9. Plots of wide-angle d-spacings (■) and inter layer spacings (●) versus the number of methylene groups between the two sulfur atoms (M) of OSP-M.

also indicate that the side chains are perpendicular to the polymer backbone [27,37]. Therefore, it is very reasonable to expect that the side chains of OTP-Ms and OSP-Ms are perpendicular to the polymer backbone axis.

Figs. 8 and 9 show the inter-layer spacings and the wide-angle d-spacings of all the polymers plotted against M. The inter-layer spacings of the polymers with $M = 5, 6, 7$ and the polymers with $M = 3, 4, 9, 12$ lies on the different lines for both OTM-Ms and OSP-Ms, and the slopes of the lines are very close. The wide-angle d-spacings of the polymers with $M = 5, 6, 7$ and the polymers with $M = 3, 4, 9, 12$ also lies on the different lines. Therefore, the position of the sulfone groups in the outer part of the side chain controls the layer structures of the polymers.

The numbers of carbon and sulfur atoms in the side chain between the outer sulfone group (denoted as ● in Fig. 10) and the backbone for the polymers with $M = 5, 6$, and 7 are 7, 8, 9, respectively. There are eight carbons in the tail part of the side-chain since the tail group is octyl. Although, we do not know the contributions of the van der Waals radius and the backbone/side chain conformations to the spacings, it is quite reasonable to say that the inter- and intra-distances (d_{inter} and d_{intra} in Fig. 10) for the polymers with $M = 5, 6, 7$ are close as shown in Fig. 10; d_{C8} is detonated as the length of the octyl tail then $d_{\text{intra}} \cong 2 \times d_{C8}$ for the polymers with $M = 5, 6, 7$. However, the d_{intra} of the polymers with $M = 3, 4, 9, 12$ is not close to the $2d_{C8}$ probably because they have partially intercalated structures (Fig. 10). Although we do not know the origin of such results, it seems like that d_{intra} or the position of the outer sulfone group controls the layer structures.

It was reported that other comb-like polymers with long alkyl side groups can have single-layer structures, double-layer structures, or intercalating double-layer structures; for example poly(alkyl acrylate)s have the double-layer structures without intercalation, while poly(alkyl methacrylate)s and poly(*N*-alkyl acrylamide)s have the intercalating double-layer structures [37]. It has been known that the layer structures are determined by the structures of the backbones units, which was already claimed by several authors [26,31,38], then the side tails just change the layer distance in a linear manner [27,33,37–44]. However, liquid crystalline poly(acrylate)s with fluoroalkyl side groups

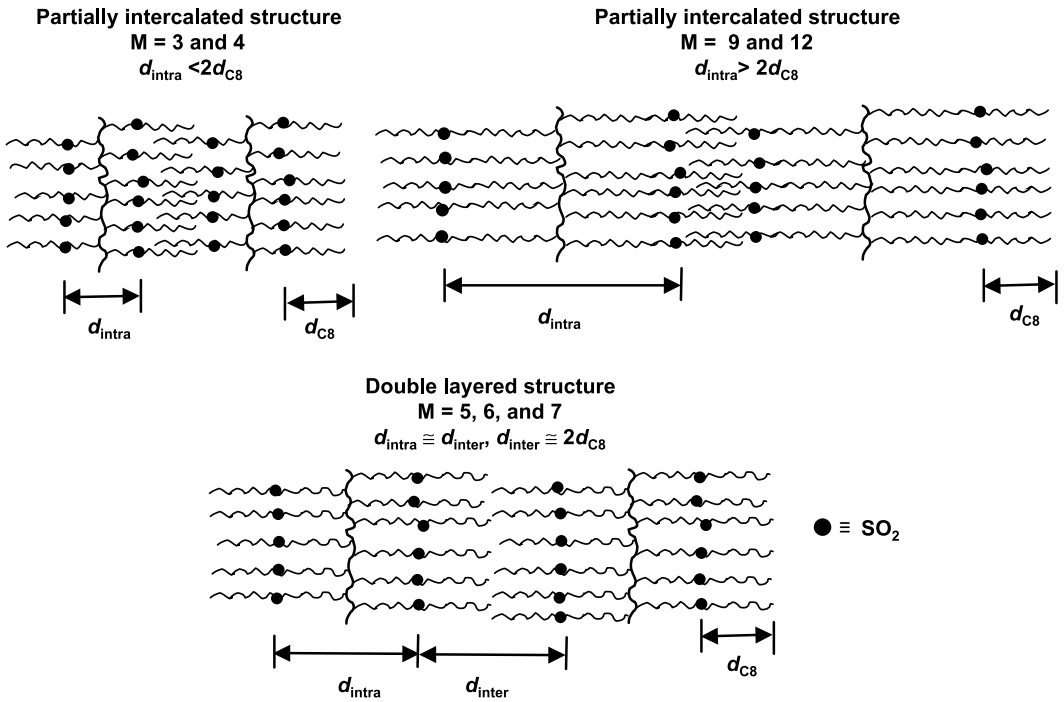

Fig. 10. Models proposed for the polymers where ● is the sulfone (SO_2) group.

showed two types of layer structures according to the side-chain length as mentioned at the end of *thermal behavior* part of this paper [33]. The liquid crystallinity of the fluorinated polymers has been ascribed to the rigidity of the fluorocarbon chains and the phase separation between the fluorocarbon units and other groups. We also can expect relatively large and small phase separation for OSP-Ms and OTP-Ms, respectively. Some chain rigidity could be expected because the side chains contain very polar sulfone groups. Because of these factors, in some degree, the role of the alkylsulfonyl groups in OTP-Ms and OSP-Ms is quite similar to that of fluoro groups; both the sulfone and fluoro groups induced mersomorphic structures. However their structural changes according to the side chain length are not the same. The layer structures of the fluorinated polymers change from single-layer to double-layer structures as the side chain lengths increase. The layer structures of OSP-Ms and OTP-Ms change from single-layer to double-layer structures, then finally return to single-layer structures again. Therefore, the effect of the dipole–dipole interactions of the sulfone groups on the ordered structures is quite unique.

4. Conclusions

((*n*-Octylsulfonyl)alkylthiomethyl)-substituted poly(oxyethylene)s (OTP-Ms) and (*n*-octylsulfonyl)alkylsulfonyl)methyl-substituted poly(oxyethylene)s (OSP-Ms), where M is the number of carbons in the alkyl group in the side chain ($M = 3, 4, 5, 6, 7, 9, 12$), were synthesized to investigate the effect of the dipole–dipole interactions of sulfone groups on the ordered phases of the polymers. POM and DSC results show that all the OTP-Ms and OSP-3 have only side chain crystalline phases, while OSP-Ms except OSP-3 have liquid crystalline phases below their isotropic temperatures, which indicates that the sulfone groups near to the oxyethylene backbone generally determine the ordered phases of the poly(oxyethylene) derivatives. X-ray results show that the polymers with $M = 5, 6, 7$ have double-layer structures and the polymers with $M = 3, 4, 9, 12$ have the intercalating double-layer structures at room temperature, which indicates the position of the dipole–dipole interactions or the sulfone group in the outer part of the side-chain determines the layer structures. Therefore, it has been shown that, in addition to hydrogen bonding, ionic interactions, metal coordinations, mesogenic groups, and hydrophilic/hydrophobic effects, the dipole–dipole interactions between the very polar sulfone groups can generate and control the ordered structures of the polymeric materials in a rather unique mechanism.

Acknowledgements

Financial support of this work by Korea Science and Engineering Foundation through Hyperstructured Organic Materials Research Center and by the Research Institute of Engineering Science (RIES) at Seoul National University is gratefully acknowledged. Soo-Young Park acknowledges financial support from Air Force Office of Scientific Research for an NRC postdoctoral research associateship.

References

[1] Isaacs L, Chin DN, Bowden N, Xia Y, Whitesides GM. In: Reinhoudt DN, editor. Supramolecular materials and technologies. New York: Wiley; 1999. p. 1–46.
[2] Lehn J-M. Supramolecular chemistry. New York: VCH; 1995. p. 89–138.
[3] Kato T, Fréchet JM. Polymeric materials encyclopedia. New York: CRC Press; 1996. p. 8158–61.
[4] Percec V, Tomazos D. In: Allen SG, editor. Comprehensive polymer science, first supplement. Oxford: Pergamon Press; 1992. p. 299–384.
[5] Ruokolainen J, Brinke G, Ikkala O, Torkkeli M, Serimaa R. Macromolecules 1996;29:3409.
[6] Muthukumar M, Ober CK, Thomas EL. Science 1997;277:1225.
[7] Ober CK, Wegner G. Adv Mater 1997;9:17.
[8] Won Y-Y, Daves HT, Bates FS. Science 1999;283:960.
[9] Zhou S, Chu B. Adv Mater 2000;12:545.
[10] Park S-Y, Farmer BL, Lee J-C. Polymer 2002;43:177.
[11] Lee J-C, Lim M-Y, Oh K, Kim YG, Lee HB, Park S-Y, Farmer BL. Polymer 2002;43:7051.
[12] Zhang T, Litt MH, Rogers CE. J Polym Sci, Polym Chem Ed 1994;32:2291.
[13] Dass NN, Date RW, Fawcett AH, McLaughlin JD, Sosanwo OA. Macromolecules 1993;26:4192.
[14] Pugh C, Kiste AL. In: Demus D, Goodby J, Gray GW, Spiess H-W, Vill V, editors. Handbook of liquid crystal, vol. 36. New York: Wiley and VCH; 1998. Chapter 3.
[15] Ciferri A. In: Ciferri A, Krigbaum WR, Meyer RB, editors. Polymer liquid crystals. New York: Academic press; 1982. p. 63–102.
[16] Sirigu A. In: Ciferri A, editor. Liquid crystallinity in polymers. New York: VCH; 1991. p. 261–313.
[17] Nelson JrRD, Lide JrDR, Maryott AA. In: Weast RC, editor. CRC handbook of chemistry and physics, 67th ed. New York: CRC Press; 1986. p. E58–9.
[18] Lee J-C, Litt MH, Rogers CE. Macromolecules 1998;31:2240.
[19] Ringsdorf H, Schneller A. Makromol Chem Rapid Commun 1982;3:557.
[20] Naciri J, Ratna BR, Baral-Tosh S, Keller P, Shashidhar R. Macromolecules 1995;28:5274.
[21] Guichard B, Noël C, Reyx D, Kajzar F. Makromol Chem Phys 1996;197:2185.
[22] Raja KS, Raghunathan VA, Ramakrisshnan S. Macromolecules 1998;31:3807.
[23] Craig AA, Imrie CT. Macromolecules 1999;32:6215.
[24] Ungar G. Polymer 1993;34:2050.
[25] Wunderich B. Thermochim Acta 1999;340–341:37.
[26] Akiyama E, Otomo M, Nagase Y, Koide N. Makromol Chem Phys 1995;190:3391.
[27] Platé NA, Shibaev VP. J Polym Sci, Macromol Rev 1974;8:117.
[28] Lee JL, Pearce EM, Kwei TK. Macromolecules 1997;30:6877.
[29] Aharoni SM. J Polym Sci, Polym Phys Ed 1980;18:1303.
[30] Watanabe J, Harkness BR, Sone M, Ichimura H. Macromolecules 1994;27:507.
[31] Rodriguez-Parada JM, Duran R, Wegner G. Macromolecules 1989;22:2507.
[32] Kricheldorf HR, Domschke A. Macromolecules 1996;29:1337.

[33] Shimizu T, Tanaka Y, Kutsumizu S, Yano S. Macromolecules 1996; 29:156.
[34] Hsu W-P, Levon K, Ho K-S, Myerson AS, Kwei TK. Macromolecules 1993;26:1318.
[35] Zheng W-Y, Levon K, Laakso J, Österholm J-E. Macromolecules 1994;27:7754.
[36] Lee J-C, Litt MH, Rogers CE. Macromolecules 1997;30:3766.
[37] Hsieh HW, Post B, Morawetz H. J Polym Sci, Polym Phys Ed 1976; 14:1241.
[38] Kim H, Park S-B, Jung JC, Zin W-C. Polymer 1996;13:2845.
[39] Dreja M, Lennartz W. Macromolecules 1999;32:3528.
[40] Tsiourvas D, Paleos CM, Skoulios A. Macromolecules 1997;30:7191.
[41] Ballauff M, Schmit GF. Mol Cryst Liq Cryst 1987;147:163.
[42] Rodriguez-Parada JM, Duran R, Wegner G. Macromolecules 1989; 22:2507.
[43] Jiao H, Goh SH, Valiyaveettil S. Langmuir 2002;18:1368.
[44] Dessipiri E, Tirrell DA, Atkins EDT. Macromolecules 1996;29:3545.